

# Giant bubbles of Fisher zeros in the quantum XY chain

Songtai Lv,<sup>1</sup> Yang Liu,<sup>2,\*</sup> Erhai Zhao,<sup>3,†</sup> Haiyuan Zou,<sup>1,4,‡</sup> and Tao Xiang<sup>5,6,§</sup>

<sup>1</sup>*Key Laboratory of Polar Materials and Devices (MOE),*

*School of Physics, East China Normal University, Shanghai 200241, China*

<sup>2</sup>*Department of Physics and Astronomy, University of California, Riverside, California 92521, USA*

<sup>3</sup>*Department of Physics and Astronomy, George Mason University, Fairfax, Virginia 22030, USA*

<sup>4</sup>*State Key Laboratory of Low-Dimensional Quantum Physics,*

*Department of Physics, Tsinghua University, Beijing 100084, China*

<sup>5</sup>*Beijing National Laboratory for Condensed Matter Physics and Institute of Physics,*

*Chinese Academy of Sciences, Beijing 100190, China*

<sup>6</sup>*School of Physical Sciences, University of Chinese Academy of Sciences, Beijing 100049, China*

We demonstrate an alternative approach based on complex-valued inverse temperature and partition function to probe quantum phases of matter with nontrivial spectra and dynamics. It leverages thermofield dynamics (TFD) to quantitatively characterize quantum and thermal fluctuations, and exploit the correspondence between low-energy excitations and Fisher zeros. Using the quantum XY chain in an external field as a testbed, we show that the oscillatory gap behavior manifests as oscillations in the long-time dynamics of the TFD spectral form factor. We also identify giant bubbles, i.e. large-scale closed lines, of Fisher-zeros near the gapless XX limit. They provide a characteristic energy scale that seems to contradict the predictions of the low energy theory of a featureless Luttinger liquid. We identify this energy scale and relate the motion of these giant bubbles with varying external field to the transfer of spectral weight from high to low energies. The deep connection between Fisher zeros, dynamics, and excitations opens up promising avenues for understanding the unconventional gap behaviors in strongly correlated many-body systems.

*Introduction.* Partition function is one of the central objects in statistical mechanics. Compared to spectral or correlation functions that directly relate to experimental observations, it receives less attention in conventional theoretical approaches to strongly correlated quantum systems. Some of these systems refuse to fall into the paradigms of order parameters and quasiparticles and therefore call for new perspectives or tools. One striking example is the so-called pseudogap in high-temperature superconductors [1–4], which is related to the lack of consensus on the phase diagram of 2D Hubbard model and related strongly correlated lattice models [5–9]. Recently, fueled by the growing interest in open and monitored quantum systems [10–14], an “unconventional” probe of quantum many body systems has been proposed. It analytically continues the partition function  $Z$  to be a function of the complex inverse temperature  $\beta = \beta_r + i\beta_i \in \mathbb{C}$ . Roughly speaking,  $Z$  accounts for both thermal and quantum fluctuations, with  $1/\beta_r$  playing the role of temperature and  $\beta_i$  as time.

The idea of complex  $\beta$  goes back to Fisher who, following the pioneering work of Lee and Yang [15, 16], showed that the location of zeros of  $Z$  on the complex  $\beta$  plane, as the solution of  $Z(\beta = \beta_r + i\beta_i) = 0$  and now referred to as Fisher zeros, can be used to identify thermodynamic phase transitions [17]. Later, in the study of quench dynamics from a given pure state, the zeros of the so-called

boundary partition function (analogous to  $Z$ ) were used to describe dynamical quantum phase transitions [18]. We have shown that the complex  $Z$  and its Fisher zeros can be applied to quantum many-body systems to characterize quantum criticality [19, 20], low-energy excitations [21], breakdowns of the eigenstate thermalization hypothesis [22], and even topological features [23]. By now, there is a surge of interest in complexified quantum many-body systems [19–31]. In this context, the best understood example of Fisher zeros is the one-dimensional transverse field Ising model (TFIM). For example, an open line of Fisher zeros extending to  $\beta_r \rightarrow \infty$  in the complex  $\beta$ -plane indicates low energy excitations, such as domain-walls, at energy scale set by  $1/\beta_i$ . A natural question then is what happens to the configuration of Fisher zeros if a system does not have well-defined quasiparticles but an enhanced, broad, incoherent spectral weight (the suppressed spectral weight then qualifies as a pseudogap)? Clearly, they should not form open lines. To address these questions, we need to go beyond TFIM to study models that feature interesting, unconventional phases that do not resemble a Fermi liquid.

These considerations motivated us to investigate the complex partition function and Fisher zeros for the 1D XY model, Eq. (1). This quantum spin system has several appealing features. First, it contains TFIM as a special limit which serves as a sanity check to ensure the result is correct. Second,  $Z$  can be computed exactly. Third, the model has a rich phase diagram including a ferromagnetic phase, a rather peculiar oscillatory phase, a gapless Luttinger liquid, and gapped disordered phase. Finally, it exhibits rich spectral structures at both low and high energies. We shall show a few surprising behav-

\* yliu1130@ucr.edu

† ezhao2@gmu.edu

‡ hyzou@phy.ecnu.edu.cn

§ txiang@iphy.ac.cn

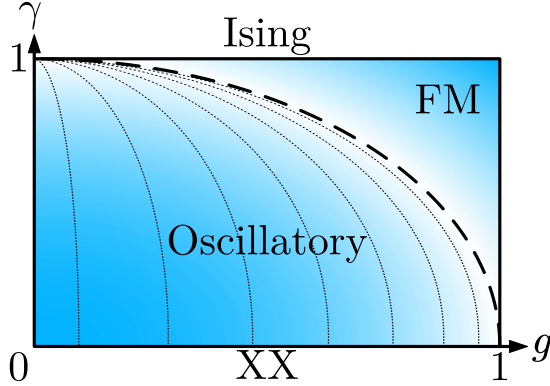


FIG. 1. Phase diagram of the quantum XY model under an external field  $g$ .  $g = 1$  is the critical line separating the FM phase from the disordered phase. The thick dashed line separates the oscillatory gap region from the FM region. The thin dashed line indicates where the gap vanishes for  $L = 16$ .  $\gamma = 1$  corresponds to the Ising limit, while  $\gamma = 0$  represents the gapless XX limit.

ions (see Fig. 4) of Fisher zeros as the model parameters are tuned, e.g., approaching various phase transitions.

*Unpacking the complex partition function  $Z$ .* Before introducing the XY model, we first recap the complex partition function can be viewed from the perspective of thermofield dynamics [32]. This will set the stage for subsequent technical discussions. If we restrict  $\beta$  to be purely imaginary, then the modulus square of  $Z$  is known as the spectral form factor  $S(t) = |Z(\beta = it)|^2$ , a popular device in quantum chaos and random matrix theory to characterize energy level statistics [33–35]. Thus spectral information is baked into  $Z$  once we introduce the imaginary part of  $\beta$ . For general  $\beta$ , we view  $Z$  as the return amplitude of a pure state once we purify the thermal ensemble. This can be done by introducing the thermofield double (TFD) state  $|\Psi(\beta_r, 0)\rangle = \sum_n e^{-\beta_r E_n/2} |n\rangle_L \otimes |n\rangle_R$  where the degrees of freedom have been doubled (the original  $L$  and its copy  $R$ ) [32]. Then  $Z(\beta_r, t) \sim \langle \Psi(\beta_r, 0) | \Psi(\beta_r, t) \rangle$ , where the inverse temperature  $\beta_r$  serves as a parameter while  $t = \beta_i$  is the real time. At large  $\beta_r$ , the oscillatory part of the normalized  $S = |Z(\beta = \beta_r + i\beta_i)/Z(\beta = \beta_r)|^2$  has two main contributions:  $2e^{-\beta_r \Delta_\infty} \cos(\Delta_\infty \beta_i)$  and  $2e^{-\beta_r \Delta_L} \cos(\Delta_L \beta_i)$ . Here  $\Delta_\infty$  is the lowest excitation gap in the thermodynamic limit, and  $\Delta_L$  is a finite-size gap satisfying  $\Delta_L < \Delta_\infty$ . If the system size  $L$  is taken to infinity first, the second term becomes negligible. In contrast, if  $L$  is kept finite and  $\beta_r$  is increased, the long-time dynamics of  $S$  will be dominated by finite-size effects. Therefore, by choosing appropriate values of  $L$ ,  $\beta_r$ , and  $\beta_i$ , one can access both the thermodynamic-limit and finite-size gap structures. A careful treatment of these limits is crucial to discuss the oscillatory phase of the XY model.

With the advancement in tensor network algorithms, the complex  $Z$  can be computed reliably for lattice spin models [36, 37] to offer a unified framework to capture

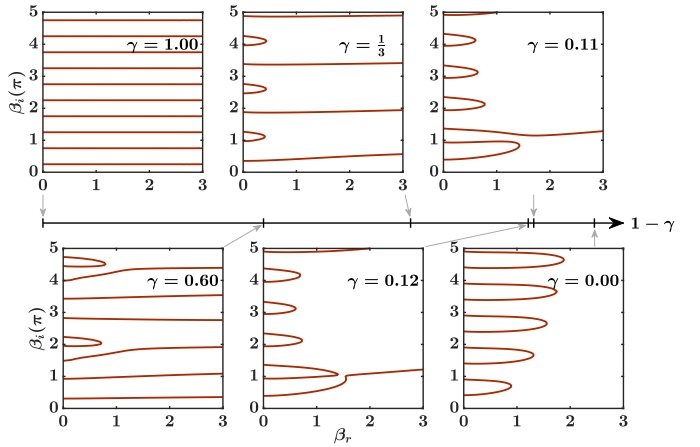


FIG. 2. Fisher zeros of the XY model without external field ( $g = 0$ ) in the thermodynamic limit for different values of  $\gamma$ . As  $\gamma$  decreases from the Ising limit ( $\gamma = 1$ ) toward the XX limit ( $\gamma = 0$ ), an upward-moving open Fisher zero line crosses over with a downward-moving closed Fisher zero line. The cases  $\gamma = 0.12$  and  $0.11$  provide the crossover example closest to the  $\beta_r$ -axis.

the competition between thermal and quantum fluctuations. In this work, we shall use the exact solutions of complex  $Z$ , in particular the asymptotic behaviors of  $S$  and the evolution of Fisher zeros, to diagnose the quantum XY model. Our main objective is to find out whether these theoretical devices yield additional insights about more “exotic” (the incommensurate phase with oscillating finite-size gaps) or “featureless” Luttinger liquids (which turn out to have rather interesting interplays of low and high energy excitations) beyond TFIM.

*Exact Fisher zeros for the 1D quantum XY model.* The Hamiltonian of the 1D XY model reads

$$H = -\sum_{j=1}^L \left[ \frac{1+\gamma}{2} \sigma_j^x \sigma_{j+1}^x + \frac{1-\gamma}{2} \sigma_j^y \sigma_{j+1}^y + g \sigma_j^z \right]. \quad (1)$$

Here  $\sigma_j^\mu$  ( $\mu = x, y, z$ ) are Pauli matrices at site  $j$ ,  $g$  is the transverse field,  $\gamma$  is the anisotropy parameter, and periodic boundary condition is assumed. As a paradigmatic example of quantum magnetism, this model has a rich phase diagram [38–40] summarized in Fig. 1. The  $g = 1$  line separates the disordered ( $g > 1$ ) from the ordered ferromagnetic phase ( $g < 1$ ). But the region bounded by the line  $\gamma^2 + g^2 = 1$  is peculiar: its spin correlation function oscillates on top of power law decay, and for finite system sizes, the gap also exhibits oscillations. As illustrated in Fig. 1 for  $L = 16$ , the gap vanishes along a set of lines in the  $g - \gamma$  plane, which become increasingly dense with larger system sizes [40]. This region is usually referred to as the oscillatory or incommensurate phase. The model reduces to TFIM along the line  $\gamma = 1$ . And for  $\gamma = 0$ , it reduces to the XX model which serves as a representative example of a gapless Luttinger liquid in the thermodynamic limit.

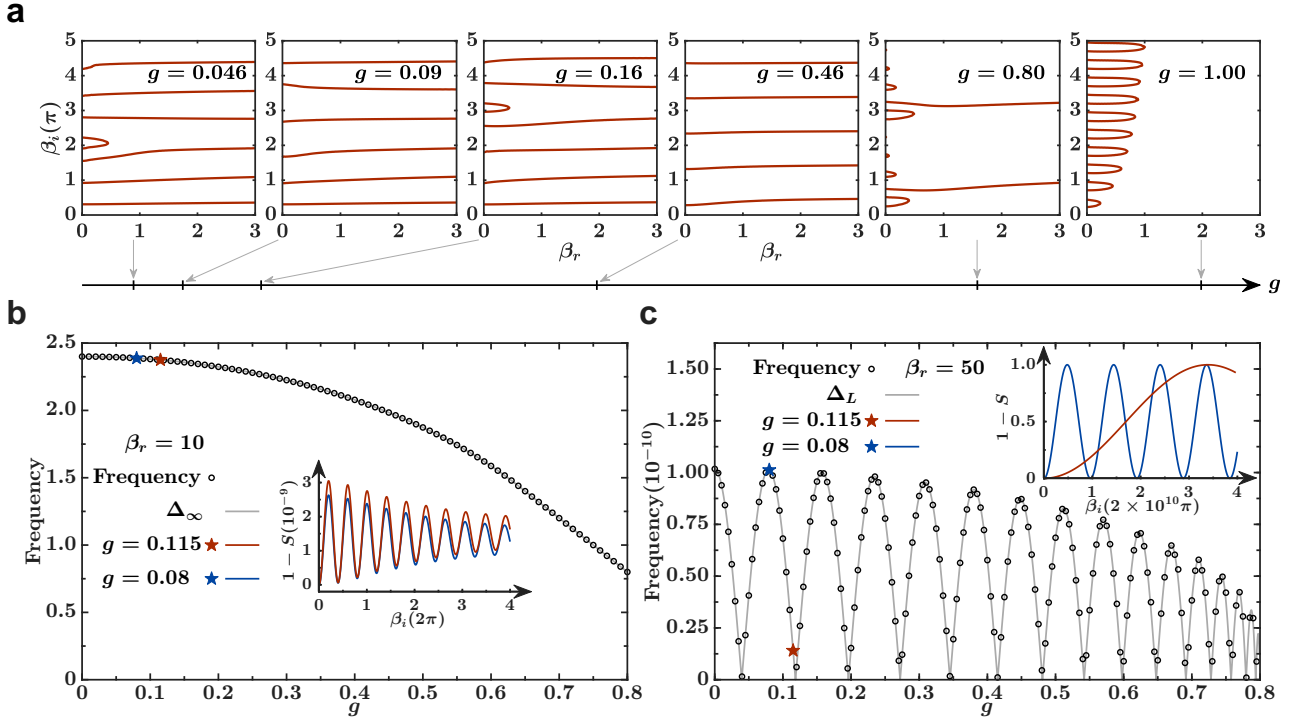


FIG. 3. Oscillatory behavior of Fisher zeros and  $S$  for  $\gamma = 0.6$ . (a) Evolution of Fisher zero configurations in the thermodynamic limit as  $g$  increases. Before reaching  $g = 1$ , the closed Fisher zero loops exhibit non-monotonic behavior, including disappearing and reappearing at  $g \lesssim 0.5$ . (b) For  $L = 32$  and  $\beta_r = 10$ , the oscillation frequency of  $S$  (black hollow dots) agrees well with  $\Delta_\infty$  (gray line). The inset shows the oscillation of  $1 - S$  with  $\beta_i$  for two nearby values  $g = 0.08$  (blue pentagram) and  $g = 0.115$  (red pentagram). (c) For  $L = 32$  and  $\beta_r = 50$ , the oscillation frequency of  $S$  (black hollow dots) matches  $\Delta_L$  (gray line). This inset shows the long-time oscillatory behavior of  $1 - S$  for the two  $g$  values from (b).

Our analysis begins by analytically continuing the exact partition function  $Z$  of the  $XY$  model to complex values of the inverse temperature  $\beta$ . Note that the exact form of  $Z$  is subtle and has not been clarified until recently [41, 42]. For  $g < 1$ , by extending the technique we used earlier to obtain the Fisher zeros of TFIM [21], we can derive the exact Fisher zeros of the  $XY$  model off the  $\beta_i$ -axis in the thermodynamic limit. They are given by the transcendental equation

$$\int_0^\pi \log |\tanh(\beta\epsilon_q)|^2 dq = 0, \quad (2)$$

where  $\epsilon_q = \sqrt{[g - \cos(q)]^2 + [\gamma \sin(q)]^2}$ . Eq. (2) is exact and one of the main results of this work.

To appreciate the form and location of Fisher zeros, let us first examine the case of zero transverse field,  $g = 0$ , as shown in Fig. 2. We observe that similar to the case of TFIM [21], the zeros congregate either to open lines or closed loops, or ‘‘bubbles’’ (only half the loops are shown as the diagram is mirror symmetric with respect to the  $\beta_i$  axis). The open lines extend to large  $\beta_r$  (low temperatures), and as we have shown earlier [21], its vertical location, i.e. the inverse of the imaginary part of the Fisher zeros ( $1/\beta_i$ ), provides a useful diagnostic measure

for the lowest energy gap of the system. As  $\gamma$  is decreased (Fig. 2), the open Fisher zero lines shift upward in the complex  $\beta$  plane accompanied by the downward movement of closed zeros. In other words, the lines rise while the bubbles sink. This is in accordance with the closing of the gap as  $\gamma$  decreases. In the limit of  $\gamma = 0$ , the system becomes gapless and the open zero lines vanish completely. This example provides another illustration that the structure change of Fisher zeros can effectively pinpoint quantum criticality.

*Short- and long-time dynamics in the oscillatory phase.* To see whether the complex  $Z$  can shed some light on the enigmatic oscillatory phase within  $\gamma^2 + g^2 < 1$ , we show in Fig. 3(a) the evolution of Fisher zeros along the cut  $\gamma = 0.6$ . Here the overall trend is that increasing  $g$  leads to an upward shift of the open zero lines and a downward movement of the closed loops (bubbles). However, in contrast to Fig. 2, the motion of the bubbles at small  $\beta_r$  values is non-monotonic: they can appear or disappear suddenly. This anomalous behavior, which is absent in TFIM, can be taken as another marker of the oscillatory phase. In other words, the oscillatory phase leaves its imprint on the Fisher zero configurations in the thermodynamic limit.

To establish a direct and quantitative connection to

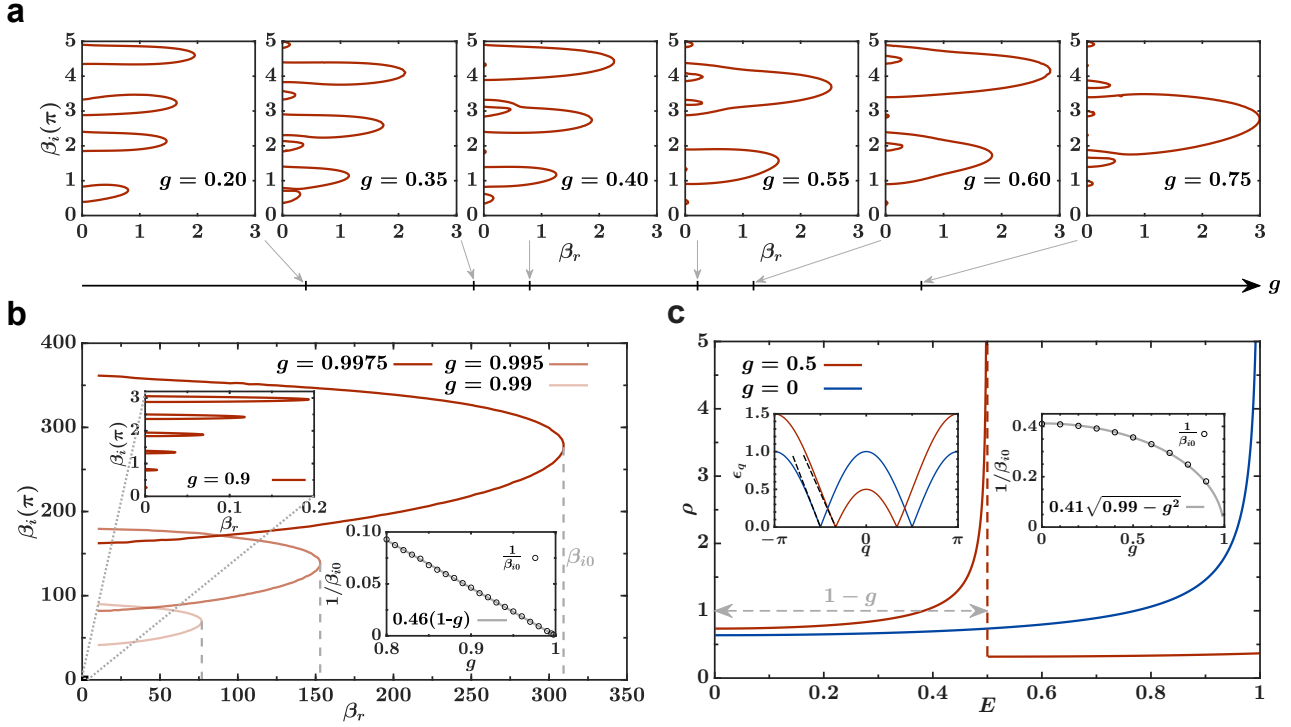


FIG. 4. Large-scale closed Fisher zero patterns at  $\gamma = 0$ . (a) For different  $g$ s, the Fisher zeros form only closed loops. As  $g$  increases, the closed zero loops exhibit a tendency to expand. (b) Near the QCP, the expansion of the large-scale closed Fisher zero loop becomes more pronounced compared to the smaller zero loops near the  $\beta_i$ -axis (upper-left inset). The lower-right inset shows that the inverse of the imaginary part ( $1/\beta_{i0}$ ) of the rightmost Fisher zero on the large loop scales linearly with  $1 - g$ . (c) The DOS diverges near  $1 - g$ , as illustrated for  $g = 0$  (blue) and  $g = 0.7$  (red), exhibiting van Hove singularities. The left inset shows the corresponding dispersion relations  $\epsilon(q)$ , where the dashed slope illustrates the Luttinger-liquid velocity, which is proportional to  $\sqrt{1 - g^2}$ . The right inset displays the dependence of  $1/\beta_{i0}$  of the open zero lines on  $g$  ( $1/\beta_{i0} \sim \sqrt{0.99 - g^2}$ ) at  $\beta_r = 100$  when a small anisotropy  $\gamma = 0.1$  is introduced.

the oscillatory gap behavior (dotted lines in Fig. 1), we further compute the normalized  $S$  for finite-size systems across the entire parameter range of  $\gamma > 0$ . As discussed earlier, both the finite-size gap ( $\Delta_L$ ) and the gap in the thermodynamic limit ( $\Delta_\infty$ ) can be extracted by taking different limits of  $\beta$  and  $L$ . In Fig. 3(b), we choose  $\beta_r = 10$  and  $L = 32$  for  $\gamma = 0.6$ . Since  $\beta_i$  plays the role of time, the short-time oscillation frequency of  $S$  gives  $\Delta_\infty$  which is in good agreement with the analytical result  $\Delta_\infty = \gamma\sqrt{(1 - \gamma^2 - g^2)/(1 - \gamma^2)}$  for  $g < 1 - \gamma^2$ , and by  $|1 - g|$  for  $g > 1 - \gamma^2$  determined from the condition  $d\epsilon_q/dq = 0$  [43]. This agreement becomes even better as both  $L$  and  $\beta_r$  increase. In this regime, adjacent values of  $g$  have only minor differences in their oscillation periods. The finite-size gap  $\Delta_L$  is extracted by fixing  $L$  using significantly larger  $\beta_r$ . An example is shown in Fig. 3(c), where huge values of  $\beta_i$  are used to show the long-time oscillation of  $S$ . The extracted  $\Delta_L$  oscillates with  $g$ , in excellent agreement with the exact solutions for  $\Delta_L$  reported in the literature [40]. In this case, even small differences in  $g$  lead to noticeable changes in the oscillation frequencies of  $S$  (see inset). Thus, the thermofield dynamics encoded in  $S$  provides unambiguous evidence

to identify the oscillatory phase in the XY model. This is the second main result.

*Giant Fisher bubbles.* Now let us focus on the XX limit at  $\gamma = 0$ , where the system remains gapless for  $g \leq 1$ . What do the Fisher zeros look like in this phase? The complex  $\beta$ -plane must contain no open zero lines; otherwise, as  $\beta_r \rightarrow \infty$ , the zeros would indicate a finite gap, contradicting the gapless nature. The exact solutions of Fisher zeros in the thermodynamic limit confirm this argument. Moreover, it shows that all zeros are in the form of closed bubbles, see Fig. 4(a). An interesting trend emerges as  $g$  is increased: in addition to a population of small bubbles near the  $\beta_i$ -axis, some bubbles grow in size by extending toward larger and larger  $\beta_r$ . As the bicritical point ( $g = 1$ ,  $\gamma = 0$ ) is approached, giant bubbles of Fisher zeros emerge to dominate the scene [Fig. 4(b)]. Its size  $\beta_{i0}$ , as measured by the imaginary part of its rightmost endpoint, diverges as  $g \rightarrow 1$ . This implies that at very low temperatures, the system exhibit a “pseudogap” scale  $\sim 1/\beta_{i0}$ . The inset of Fig. 4(b) shows that  $1/\beta_{i0}$  scales linearly with  $1 - g$ . What sets this energy scale with enhanced spectral weight?

The low-energy physics of the XX model at  $\gamma = 0$  can

be effectively described by a Luttinger liquid with a linear dispersion  $\epsilon(k) = v_F(k - k_F)$  around the Fermi points. This theory does not possess any characteristic energy scale other than the energy cutoff. To understand the pseudogap scale, we must go beyond the Luttinger description by considering the full energy-momentum dispersion  $\epsilon_q$  of quasiparticles which are collective excitations of interacting spins. As shown in Fig. 4(c), the band-edge extrema as a part of the “high-energy” physics give rise to van Hove singularities, i.e. divergence in the density of states (DOS)  $\rho(E) = \sum_{q: \epsilon_q=E} |d\epsilon_q/dq|^{-1}/2\pi$ , at energy  $\epsilon_0 = (1 - g)$ . This scaling behavior agrees with  $1/\beta_{i0} \propto (1 - g)$  observed from Fig. 4(b). Therefore, we can trace the origin of the pseudogap to the van Hove singularity. When  $g \rightarrow 1$ , the Fermi points move toward the band edge at small  $q$ . The result is a crossover where the separation between low- and high-energy features becomes ill-defined. The van Hove singularity merges with Fermi points with vanishing Fermi velocity  $v_F \sim \sqrt{1 - g^2}$ . On the complex plane, this process manifests itself as giant bubbles of Fisher zeros of ever increasing size.

To further check the validity of this interpretation, we investigate what happens at small  $\gamma$  when the system is driven away from the XX limit. Finite  $\gamma$  opens a gap,  $\Delta_{\text{inf}} \sim \gamma v_F$ . Thus, we predict that the open Fisher line associated with gap bends back and crosses over with the giant bubble. Moreover, The size  $1/\beta_{i0}$  of this open Fisher line should scale with  $v_F \propto \sqrt{1 - g^2}$  at large  $\beta_r$ . This is indeed what we observe from the numerical fit in the right inset of Fig. 4(c), where  $\gamma = 0.1$  and  $\beta_r = 100$ . Note that these giant bubbles are absent in TFIM. The theoretical discovery and understanding of these giant

bubbles near the XX limit, including their correlation and scaling with characteristic energy scales in the spin system, are the third main results of this work.

*Summary and outlook.* Our detailed analysis confirms that complex partition function offers an effective tool for analyzing the thermal and dynamical properties of the 1D XY model. By varying  $\beta_r$  and  $\beta_i$  and investigating the Fisher zeros and thermofield dynamics (through  $S$ ), we accurately capture the oscillatory finite-size gap behavior. In the thermodynamic limit, we uncover a distinctive class of giant bubbles (large-scale closed lines of Fisher zeros) near the critical line. We further demonstrate that the evolution of these bubbles with varying external field offers an intuitive yet sensitive probe for the transfer of spectral weight within the Luttinger liquid phase. Since the pseudogap phenomenon [44–47] is characterized by a redistribution of the spectral weight, we conjecture that Fisher zeros and thermofield dynamics may offer a new perspective for exploring the intricate many-body physics related to unconventional gap behaviors. Our approach outlined here can be extended to 2D strongly interacting models for which the complex-valued partition functions cannot be solved exactly but can be evaluated to high precision by tensor network algorithms [36, 37].

*Acknowledgments.* We thank Jiansong Pan, Fan Yang, and Xuefeng Zhang for helpful discussions. H.Z. is supported by the National Natural Science Foundation of China (Grant No. 12274126) and Open Research Fund Program of the State Key Laboratory of Low-Dimensional Quantum Physics. E.Z. acknowledges the support from NSF Grant PHY-206419, and AFOSR Grant FA9550-23-1-0598.

---

[1] B. Keimer, S. A. Kivelson, M. R. Norman, S. Uchida, and J. Zaanen, From quantum matter to high-temperature superconductivity in copper oxides, *Nature* **518**, 179 (2015).

[2] T. Timusk and B. Statt, The pseudogap in high-temperature superconductors: an experimental survey, *Reports on Progress in Physics* **62**, 61 (1999).

[3] J. Tallon and J. Loram, The doping dependence of  $t^*$  – what is the real high- $t_c$  phase diagram?, *Physica C: Superconductivity* **349**, 53 (2001).

[4] P. A. Lee, N. Nagaosa, and X.-G. Wen, Doping a mott insulator: Physics of high-temperature superconductivity, *Reviews of Modern Physics* **78**, 17 (2006).

[5] X. G. Wen and P. A. Lee, Theory of underdoped cuprates, *Physical Review Letters* **76**, 503 (1996).

[6] C. M. Varma, Theory of the pseudogap state of the cuprates, *Phys. Rev. B* **73**, 155113 (2006).

[7] K.-Y. Yang, T. M. Rice, and F.-C. Zhang, Phenomenological theory of the pseudogap state, *Phys. Rev. B* **73**, 174501 (2006).

[8] M. Qin, C.-M. Chung, H. Shi, E. Vitali, C. Hubig, U. Schollwöck, S. R. White, and S. Zhang (Simons Collaboration on the Many-Electron Problem), Absence of superconductivity in the pure two-dimensional hubbard model, *Phys. Rev. X* **10**, 031016 (2020).

[9] H. Xu, C.-M. Chung, M. Qin, U. Schollwöck, S. R. White, and S. Zhang, Coexistence of superconductivity with partially filled stripes in the hubbard model, *Science* **384**, 10.1126/science.adh7691 (2024).

[10] M. P. Fisher, V. Khemani, A. Nahum, and S. Vijay, Random quantum circuits, *Annual Review of Condensed Matter Physics* **14**, 335 (2023).

[11] Y. Li, X. Chen, and M. P. A. Fisher, Quantum zeno effect and the many-body entanglement transition, *Phys. Rev. B* **98**, 205136 (2018).

[12] B. Skinner, J. Ruhman, and A. Nahum, Measurement-induced phase transitions in the dynamics of entanglement, *Phys. Rev. X* **9**, 031009 (2019).

[13] A. Chan, R. M. Nandkishore, M. Pretko, and G. Smith, Unitary-projective entanglement dynamics, *Phys. Rev. B* **99**, 224307 (2019).

[14] S. Basu, D. P. Arovas, S. Gopalakrishnan, C. A. Hooley, and V. Oganesyan, Fisher zeros and persistent temporal oscillations in nonunitary quantum circuits, *Phys. Rev. Res.* **4**, 013018 (2022).

[15] C. N. Yang and T. D. Lee, Statistical theory of equations

of state and phase transitions. i. theory of condensation, *Physical Review* **87**, 404 (1952).

[16] T. D. Lee and C. N. Yang, Statistical theory of equations of state and phase transitions. ii. lattice gas and ising model, *Physical Review* **87**, 410 (1952).

[17] M. Fisher and W. Brittin, Statistical physics, weak interactions, field theory, Lectures in Theoretical Physics (Boulder: University of Colorado Press) vol VIIC (1965).

[18] M. Heyl, A. Polkovnikov, and S. Kehrein, Dynamical quantum phase transitions in the transverse-field ising model, *Phys. Rev. Lett.* **110**, 135704 (2013).

[19] Y. Liu, S. Lv, Y. Meng, Z. Tan, E. Zhao, and H. Zou, Exact fisher zeros and thermofield dynamics across a quantum critical point, *Phys. Rev. Res.* **6**, 043139 (2024).

[20] Y. Liu, E. Zhao, and H. Zou, From complexification to self-similarity: New aspects of quantum criticality, *Chinese Physics Letters* **41**, 100501 (2024).

[21] Y. Liu, S. Lv, Y. Yang, and H. Zou, Signatures of quantum criticality in the complex inverse temperature plane, *Chinese Physics Letters* **40**, 050502 (2023).

[22] Y. Meng, S. Lv, Y. Liu, Z. Tan, E. Zhao, and H. Zou, Detecting many-body scars from fisher zeros, *Phys. Rev. Lett.* **135**, 070402 (2025).

[23] Y. Meng, Y. Liu, E. Zhao, and H. Zou, Topological feature of real-time fisher zeros (2025), [arXiv:2504.01824](https://arxiv.org/abs/2504.01824).

[24] T. Kist, J. L. Lado, and C. Flindt, Lee-yang theory of criticality in interacting quantum many-body systems, *Phys. Rev. Res.* **3**, 033206 (2021).

[25] H. Li, X.-H. Yu, M. Nakagawa, and M. Ueda, Yang-lee zeros, semicircle theorem, and nonunitary criticality in bardeen-cooper-schrieffer superconductivity, *Phys. Rev. Lett.* **131**, 216001 (2023).

[26] X.-Y. Ouyang, Q.-J. Ye, and X.-Z. Li, Complex phase diagram and supercritical matter, *Phys. Rev. E* **109**, 024118 (2024).

[27] J. Liu, S. Yin, and L. Chen, Imaginary-temperature zeros for quantum phase transitions, *Phys. Rev. B* **110**, 134313 (2024).

[28] D.-Z. Li, X. Wang, and X.-B. Yang, Low-temperature series expansion of the square-lattice ising model: A study based on fisher zeros, *Phys. Rev. B* **111**, 155432 (2025).

[29] B. S. Shastry, Partition function zeros of quantum many-body systems, *Phys. Rev. E* **112**, 024106 (2025).

[30] J. Wang, E. Lv, X. Li, Y. Jin, and W. Li, Quantum supercritical crossover with dynamical singularity, *Phys. Rev. B* **112**, 195120 (2025).

[31] T.-Y. Gu and G. Sun, Fidelity zeros and lee-yang theory of quantum phase transitions, *Phys. Rev. B* **113**, 014417 (2026).

[32] Y. Takahashi and H. Umezawa, Thermo field dynamics, *International journal of modern Physics B* **10**, 1755 (1996).

[33] J. S. Cotler, G. Gur-Ari, M. Hanada, J. Polchinski, P. Saad, S. H. Shenker, D. Stanford, A. Streicher, and M. Tezuka, Black holes and random matrices, *Journal of High Energy Physics* **2017**, 1 (2017).

[34] A. del Campo, J. Molina-Vilaplana, and J. Sonner, Scrambling the spectral form factor: Unitarity constraints and exact results, *Phys. Rev. D* **95**, 126008 (2017).

[35] Y. Liao, A. Vikram, and V. Galitski, Many-body level statistics of single-particle quantum chaos, *Phys. Rev. Lett.* **125**, 250601 (2020).

[36] Z. Y. Xie, J. Chen, M. P. Qin, J. W. Zhu, L. P. Yang, and T. Xiang, Coarse-graining renormalization by higher-order singular value decomposition, *Phys. Rev. B* **86**, 045139 (2012).

[37] A. Denbleyker, Y. Liu, Y. Meurice, M. P. Qin, T. Xiang, Z. Y. Xie, J. F. Yu, and H. Zou, Controlling sign problems in spin models using tensor renormalization, *Phys. Rev. D* **89**, 016008 (2014).

[38] E. Barouch and B. M. McCoy, Statistical mechanics of the hexymodel. ii. spin-correlation functions, *Physical Review A* **3**, 786 (1971).

[39] C. Hoeger, G. v. Gehlen, and V. Rittenberg, Finite-size scaling for quantum chains with an oscillatory energy gap, *Journal of Physics A: Mathematical and General* **18**, 1813 (1985).

[40] M. Okuyama, Y. Yamanaka, H. Nishimori, and M. M. Rams, Anomalous behavior of the energy gap in the one-dimensional quantum *xy* model, *Phys. Rev. E* **92**, 052116 (2015).

[41] M. Białożycy, F. Gómez-Ruiz, and A. del Campo, Exact thermal properties of free-fermionic spin chains, *SciPost Physics* **11**, 10.21468/scipostphys.11.1.013 (2021).

[42] F. Franchini, An introduction to integrable techniques for one-dimensional quantum systems (2017), (Springer).

[43] T. Maciazek and J. Wojtkiewicz, On the phase diagram of the anisotropic *xy* chain in transverse magnetic field, *Physica A: Statistical Mechanics and its Applications* **441**, 131 (2016).

[44] E. Papaal and A. M. Tsvelik, A pseudogap in the single-particle density of states of a tomonaga-luttinger liquid (2000), [arXiv:cond-mat/0004007](https://arxiv.org/abs/cond-mat/0004007).

[45] Q. Chen, J. Stajic, S. Tan, and K. Levin, Bcs-bec crossover: From high temperature superconductors to ultracold superfluids, *Physics Reports* **412**, 1 (2005).

[46] E. J. Mueller, Review of pseudogaps in strongly interacting fermi gases, *Reports on Progress in Physics* **80**, 104401 (2017).

[47] Q. Chen, Z. Wang, R. Boyack, S. Yang, and K. Levin, When superconductivity crosses over: From bcs to bec, *Rev. Mod. Phys.* **96**, 025002 (2024).